miR181b-3p and its target importin α5 regulate TLR4 signaling in Kupffer cells and liver injury in mice in response to ethanol

Paramananda Saikia[1,3,*], **Damien Bellos**[1,3,*], **Megan R. McMullen**[1], **Katherine A. Pollard**[1], **Carol de la Motte**[1,3], and **Laura E. Nagy**[1,2,3]

[1]Center for Liver Disease Research, Department of Pathobiology, Cleveland Clinic, Cleveland, Ohio

[2]Center for Liver Disease Research, Department of Gastroenterology, Cleveland Clinic, Cleveland, Ohio

[3]Department of Molecular Medicine, Case Western Reserve University, Cleveland, Ohio

Abstract

Increased inflammatory signaling by Kupffer cells contributes to alcoholic liver disease (ALD). Here we investigated the impact of small-specific sized hyaluronic acid of ~35kD (HA35) on ethanol-induced sensitization of Kupffer cells, as well as ethanol-induced liver injury in mice. Un-biased analysis of microRNA (miRNA) expression in Kupffer cells identified miRNAs regulated by both ethanol and HA35. TLR4-mediated signaling was assessed in primary cultures of Kupffer cells from ethanol- and pair-fed rats after treatment with HA35. Female C57BL6/J mice were fed ethanol or pair-fed control diets and treated or not with HA35. TLR4 signaling was increased in Kupffer cells by ethanol; this sensitization was normalized by *ex vivo* treatment with HA35. Next Generation Sequencing of Kupffer cell miRNA identified miRNA181b-3p as sensitive to both ethanol and HA35. Importin α5, a protein involved in p65 translocation to the nucleus, was identified as a target of miR181b-3p; importin α5 protein was increased in Kupffer cells from ethanol-fed rats, but decreased by HA35 treatment. Overexpression of miR181b-3p decreased importin α5 expression and normalized LPS-stimulated TNFα expression in Kupffer cells from ethanol-fed rats. In a mouse model of ALD, ethanol feeding decreased miR181b-3p in liver and increased expression of importin α5 in non-parenchymal cells. Treatment with HA35 normalized these changes and also protected mice from ethanol-induced liver and intestinal injury.

Conclusions—miR181b-3p is dynamically regulated in Kupffer cells and mouse liver in response to ethanol and treatment with HA35. miR181b-3p modulates expression of importin α5 and sensitivity of TLR4-mediated signaling. To our knowledge, this study is the first to identify a miR181b-3p→importin α5 axis in regulating inflammatory signaling pathways in hepatic macrophages.

Address correspondence to: Laura E Nagy, Cleveland Clinic, Lerner Research Institute/NE40, 9500 Euclid Ave, Cleveland OH 44195, Phone 216-444-4120, Fax 216-636-1493, nagyL3@ccf.org.
*Indicates equal contribution

Keywords

alcoholic liver disease; Kupffer cells; Next Generation Sequencing; importin family; hyaluronic acid

---

Alcoholic liver disease is a multi-staged disease involving inflammation and oxidative stress in the liver resulting from both the direct and indirect effects of heavy ethanol consumption (1, 2). Several pathogenic mechanisms have been identified in ethanol-induced liver injury; activation of hepatic macrophages has emerged as a central integrator of multiple signals leading to injury. Ethanol disrupts the intestinal barrier, promoting the translocation of lipopolysaccharide (LPS) and other Pathogen Associated Molecular Patterns (PAMPs) into the portal circulation (3, 4). Furthermore, ethanol-induced hepatocyte injury releases Danger Associated Molecular Patterns (DAMPs) into the microenvironment, which can in turn activate hepatic macrophages and other immune cells (5). Together with the oxidative stress resulting from ethanol metabolism, increased expression of pro-inflammatory cytokines and chemokines promotes ethanol-induced hepatocellular injury (4).

In addition to increased concentrations of PAMPs and DAMPs, TLR4-mediated signaling is also sensitized in Kupffer cells after ethanol exposure; ethanol enhances TLR4-stimulated activation of MAPK family members and NFκB, leading to both increased transcription and mRNA stability of inflammatory mediators (4, 6). This ethanol-induced sensitization contributes to an ongoing state of chronic inflammation in the liver, rather than a naturally resolving inflammatory response. The molecular mechanisms for this increased sensitivity of Kupffer cells to activation, as well as their failure to resolve their activation state, are not well understood.

MicroRNAs (miRNA), a group of non-protein coding RNA of 20–22 nucleotides long, play an important role in modulating macrophage activity and plasticity (7). Several specific miRNAs have been identified that likely contribute to ethanol-induced liver injury (8). For example, up-regulation of miR155 after chronic ethanol contributes to the stabilization of TNFα mRNA in hepatic macrophages (9). Therefore, understanding the interaction between ethanol and miRNA in hepatic macrophages is important for understanding the progression of injury and identifying potential therapeutic targets.

During the response to tissue injury, simple glycans, such as hyaluronan (HA), play an important role in both the generation and resolution of inflammatory responses (10, 11). The concentration of HA is increased in the circulation of patients with ALD (12); however, the specific sizes of the HA generated are not known. HA can have both pro- and anti-inflammatory impact during the response to injury, dependent on the size and matrix structure of the HA molecules, as well as cell and tissue-specific interactions with HA binding proteins and receptors (13). Exogenous HA of specific sizes can dampen inflammatory responses (14, 15). For example, mice pretreated with HA <500kD are resistant to LPS-induced septic responses through a mechanism dependent on CD44 and TLR4 (15). In the intestine, the production and degradation of HA in the surrounding matrix regulates inflammatory responses and specific-sized HA promotes gut barrier integrity (16, 17) as well as homeostatic compartmentalization of gut bacteria (18).

Given the potential anti-inflammatory effects of HA, combined with its ability to protect the integrity of the intestinal barrier, we hypothesized that small specific-sized HA molecules could have protective effects in the face of ethanol exposure. Using primary cultures of Kupffer cells from ethanol- and pair-fed rats, we found that HA35 normalized TLR4 signaling after ethanol exposure. Using Next Generation Sequencing (NGS), we identified individual miRNAs that were down-regulated in Kupffer cells after ethanol feeding and restored by treatment with HA35. Gene target analysis identified 3 miRNAs that fulfilled these criteria; all three of these miRNA regulate proteins involved in nuclear-cytoplasmic shuttling. One of these miRNAs, miR181b-3p regulated expression of importin α5, an important part of the nuclear transport machinery for the p65 subunit of NFκB. Ectopic expression of miR181b-3p normalized LPS-stimulated TNFα expression in Kupffer cells from ethanol-fed rats. Short-term ethanol feeding to mice also decreased miR181b-3p expression in liver and increased importin α5 expression in non-parenchymal cells. Treatment with HA35 during ethanol feeding normalized these responses and also prevented ethanol-induced liver injury. HA35 also prevented ethanol-induced leakage of intestinal endotoxins into the portal circulation and disruption of tight junction complexes in the proximal colon. In summary, here we have taken an un-biased approach to identify miR181b-3p and importin α5 as contributors to the sensitization of TLR4 signaling in Kupffer cells after ethanol feeding, as well as to the pathophysiology of ethanol-induced liver injury. Treatment with HA35 was able to normalize miR181b-3p and importin α5 expression and prevent ethanol-induced injury.

Materials and Methods

Chronic ethanol feeding to rats and isolation and culture of Kupffer cells

All procedures involving animals were approved by the Institutional Animal Care and Use Committee at the Cleveland Clinic. Adult male Wistar rats weighing 140–150 g were purchased from Envigo (Indianapolis, IN). Chronic ethanol feeding to rats and the isolation and culture of Kupffer cells were performed as previously described (19). Briefly, rats were allowed free access to the Lieber-Decarli high-fat liquid diet (#710260, Dyets, Bethlehem, PA) for 2 days. Rats were weight matched and then randomly assigned to pair-fed or ethanol-fed groups. Ethanol-fed rats were allowed free access to a liquid diet containing 17% of the calories (3.3% vol/vol) from ethanol for 2 days and then a liquid diet containing 35% of the calories (6.7% vol/vol) from ethanol for 4 weeks. Control rats were pair-fed a liquid diet in which maltose dextrin was substituted isocalorically for ethanol over the entire feeding period. Kupffer cells were isolated and cultured, as previously described (19). After 18 hours in culture, cells were treated with or without 100μg/ml small-specific-sized HA (Lifecore Biomedical, LLC, Chaska, MN) for 5 h. HAs are identified by their average molecular weight, i.e. HA35 has an average molecular weight of 35kD. Kupffer cells were then challenged with 10 ng/mL LPS (*Escherichia Coli* strain 0111:B4, Sigma-Aldrich), as indicated in the figure legends. For experiments using miRNA mimics, Kupffer cells were transfected using the Amaxa mouse macrophage Nucleofector kit using the Y-001 program (Lonza, Cologne, Germany), as previously reported (20). After nucleofection, cells retained sensitivity to LPS, ethanol and HA35; however, the level of expression of TNFα was lower

than in non-transfected cells. Sequences of miRNAs probes and mimics are listed in Supplemental Table 1.

Short-term ethanol feeding to mice

Ten to twelve week old female C57BL6/J mice were purchased from Jackson Laboratories (Bar Harbor, ME) and allowed free access to a Lieber-DeCarli liquid diet containing ethanol or a pair-fed control diet that isocalorically substituted maltose dextrin for ethanol as previously described (21). Mice were housed two per micro-isolator cage and were maintained in a temperature regulated facility with a 12 hour light-dark cycle, with Nylabones provided for environmental enrichment. Mice were introduced to the control liquid diet for two days and then weight matched and randomly distributed to ethanol or control diets. Ethanol diets were initiated at 1% (v/v) for two days and then increased to 6% (v/v) or 32% of total calories for an additional two days. During the last three days of feeding, mice were gavaged with 15 mg/kg HA35 in sterile saline or an equivalent volume of saline (vehicle) at 1:30 pm. The morning after the last HA35 treatment, ethanol- and pair-fed mice were anesthetized and samples collected prior to euthanasia. Blood was taken from the hepatic portal vein in capillary tubes for AST or directed into borosilicate culture tubes for endotoxin testing. The livers were perfused, excised and sectioned for RNA, protein and histology. Proximal colon was sectioned and fixed in Histochoice (Amresco, Solon, OH). In one experiment, livers were perfused with saline and then digested in collagenase for isolation of non-parenchymal cells by differential centrifugation (22).

microRNA preparation and NGS

Small RNA was isolated using miRNeasy Mini Kit (Qiagen, Germantown, MD) and sequenced following the Small RNA Sample Preparation Protocol (Illumina, San Diego, USA). The library was prepared from 10 ng of total RNA per sample according to the manufacturers instructions (TruSeq, Small RNAKit, Illumina). Single-stranded cDNAs were created with SuperScriptII Reverse Transcriptase and double-stranded cDNAs generated by PCR using adapter specific primers. Purified libraries were quantified and qualified using the High Sensitivity DNA Kit on a 2100 Bioanalyzer (Agilent Technologies, Böblingen, Germany). Sequencing of the libraries was carried out at the Genomic Core Facility (Cleveland Clinic) utilizing HiSeq2000 (Illumina). After sequencing, the data were obtained in Illumina FASTQ format (Illumina). The data were analyzed using NGS small RNA sequence analysis software (version 2.5.1) using the rat build rn4MiRNA program (see Supplemental Figure 1 for description of data analysis pipeline). NGS data have been deposited in NCBI's Gene Expression Omnibus and are awaiting assignment of their accession number.

Molecular and biochemical assays

Total RNA was isolated, reverse transcribed and qRT-PCR amplification was performed, as previously described (20). The relative amount of target mRNA was determined using the comparative threshold (Ct) method by normalizing target mRNA Ct values to those of 18S. Western blot analysis of Kupffer cell, liver or intestinal homogenates was performed as previously described (21). Antibody sources are listed in Supplemental Table 1. Plasma samples were analyzed for aspartate aminotransferase (AST) using the AST-SL (Sekisui

Diagnostics, Lexington, MA). Triglycerides were assessed in whole liver using the Triglyceride Reagent Set (Point Scientific, Canton, MI) (21).

Immunohistochemistry

Formalin (liver) or Histochoice (proximal colon)-fixed paraffin-embedded sections were de-paraffinized and used to assess M30 cytoDEATH (Roche, 12140322), TUNEL (Merck Millipore, S7111) and phospho-p65 in liver (23) or ZO-1 and occludin in proximal colon (24). Staining for Oil Red O was performed using sections cut from frozen liver in OCT. Nuclei were labeled using Vectashield with DAPI or hematoxylin. Coded slides were imaged and semi-quantification was performed using Image Pro-plus (Media Cybernetics, Silver Springs, MD).

Endotoxin assay

All glassware used for endotoxin collection and detection was rendered endotoxin-free by baking at 225°C overnight(25). Plasma was isolated from portal blood by centrifugation at 150g for 10min at 4°C and then stored at −80°C until testing. Endotoxin Sample Preparation Kit (ESP) (BioDtech (Birmingham, AK) was used according to the manufacturer's instruction and endotoxin concentration measured with Pyrogent-5000 assay (Lonza, Basel, Switzerland). As a control, endotoxin standards were spiked into ESP-treated plasma samples to confirm endotoxin recovery within the manufacturer's acceptable range (50–200%).

Statistical analysis

Values shown in all figures represent means + SEM. Data was analyzed by Analysis of Variance using a general linear model and least square means test for comparisons between groups (SAS, Carey, IN). Normal distribution of the data was assessed using the Shapiro-Wilk test and data was log-transformed as necessary to obtain a normal distribution. If the data were not normally distributed, non-parametric analysis was performed using PRISM software. Statistical difference between groups was determined at $p < 0.05$. Different alphabetical superscripts denote significant difference between groups.

Results

Small-sized HA fragments differentially regulated LPS-stimulated TNFα mRNA expression in primary Kupffer cells from ethanol- and pair-fed rats

Kupffer cell activation is an early event during progression of ALD, resulting from increased exposure to PAMPs, as well as a sensitization of Kupffer cells to TLR4-dependent cytokine production (4, 6). Kupffer cells are also likely exposed to a variety of DAMPs as a result of hepatocellular injury. One potentially important DAMP is hyaluronic acid; however, depending on its size, small specific-sized HAs can have either pro- or anti-inflammatory effects. In this study, we screened a series of small specific-sized HA fragments for their pro- and/or anti-inflammatory effects on Kupffer cells isolated from pair- and ethanol-fed rats. Kupffer cells were pre-treated with HA fragments of different sizes for 5 h and then challenged with LPS. Expression of TNFα was increased in response to LPS; Kupffer cells from ethanol-fed rats expressed greater amounts of TNFα compared to cells from pair-fed

rats (Figure 1A). HA7, HA12, HA59 and HA74 increased TNFα expression to varying degrees in Kupffer cells from pair-fed, but not ethanol-fed rats (Figure 1A). In contrast, HA35 completely normalized the sensitization of Kupffer cells from ethanol-fed rats, without affecting TNFα expression in pair-fed (Figure 1A). This protection was not specific for LPS-stimulated TNFα; HA35 also normalized LPS-stimulated expression of IL-6 and CXCL10 mRNA in Kupffer cells from ethanol-fed rats (Figure 1B/C). Taken together, these data suggest that HA35 normalized TLR4-mediated expression of cytokines mediated via both MyD88- and TRIF-dependent pathways.

NGS of miRNA identified miR181b-3p as a potential negative regulator of TLR4 signaling in Kupffer cells from ethanol-fed rats

There is a growing appreciation that miRNAs are critical regulators of TLR4 signaling (26). Therefore, using NGS of miRNAs to screen for potential regulators of TLR4 signaling, we identified miRNAs whose expression was down-regulated in Kupffer cells from ethanol-fed rats and, in turn, restored by *ex vivo* treatment with HA35. Ethanol feeding down-regulated 30 miRNAs by more than two-fold (Figure 2A, Suppl Table 2 and Suppl Figure 2). Of these miRNAs, HA35 treatment normalized the expression of 3 miRNAs (Figure 2A and Suppl Table 3). Gene targeting analysis of the 30 down-regulated miRNAs revealed that these miRNAs predominantly targeted pathways involved in nuclear-cytoplasmic shuttling, NFκB and inflammation (Supplemental Figure 2). Interestingly, the 3 miRNAs whose expression was restored by HA35 were all found to be involved in the nuclear-cytoplasmic shuttling pathway (Figure 2B), regulating expression of KPNA4 (importin α3), KPNA1 (importin α5) and TNPO1 (transportin 1) (Figure 2B).

Of the 3 reciprocally regulated miRNAs, miR181b-3p (also termed miR181b-1*) was the most highly down-regulated by ethanol; the NGS analysis revealed that expression of miR181b-3p was reduced more than 4-fold in response to ethanol (Suppl Table 2). Regulation of miR181b-3p by ethanol and HA35 was confirmed by qRT-PCR (Figure 2C). If the impact of HA35 on LPS-stimulated TNFα expression was dependent on miR181b-3p, then expression of a miR181b-3p mimic should model the effects of HA35. Transfection of Kupffer cells with miR181b-3p mimic, but not a control miRNA mimic, normalized the sensitivity of Kupffer cells from ethanol-fed rats to challenge with LPS, reducing TNFα expression to that of Kupffer cells from pair-fed controls (Figure 2D). Taken together, these data identified miR181b-3p as an important mediator of the anti-inflammatory effects of HA35 in Kupffer cells from ethanol-fed rats.

miR181b-3p regulates the expression of importin α5 and translocation of p65 subunit of NFκB in Kupffer cells

The bioinformatics tools TargetScan (targetscan.org), as well as miRDB (Mirdb.org) (27), identified importin α5 as a miR181b-3p target. Importin α5 is an importin α family member involved in the nucleocytoplasmic transport of cellular proteins expressing nuclear localization signals (28). Importin α family members interact with importin β proteins and RAN-GTPases to mediate the transport of cargos through the nuclear pore complex (28). Of particular relevance to TLR4-mediated signaling, importin α family members mediate the translocation of NFκB subunits to the nucleus; different importin α family members exhibit

varied sensitivities to binding different NFκB homo/heterodimers (28). Importin α5 is known to mediate translocation of NFκB subunits in leukocytes (29). Since chronic ethanol feeding increases TLR4-stimulated NFκB activity (4), we investigated the impact of ethanol feeding and HA35 on expression of importin α5 and nuclear translocation of p65 in Kupffer cells. Importin α5 protein expression was increased in Kupffer cells from ethanol-fed rats compared to pair-fed (Figure 3A/B); treatment with HA35 (Figure 3A) or overexpression of a miR181b-3p mimic (Figure 3B) reduced expression of importin α5 in Kupffer cells from ethanol-fed, but not pair-fed rats (Figure 3A/B). Nuclear translocation of the p65 subunit of NFκB, assessed via co-localization with DAPI nuclear staining, was increased by LPS in Kupffer cells from both pair-fed and ethanol-fed rats. Nuclear localization of p65 was stronger in Kupffer cells from ethanol-fed rats and reduced in cell treated with HA35 (Figure 3C/D).

Regulation of miR181b-3p and importin α5 expression in an *in vivo* mouse model of ethanol exposure

Short-term ethanol feeding to mice decreased expression of miR181b-3p in whole liver; HA35 treatment prevented this decrease, increasing the expression of miR181b-3p above that of pair-fed controls (Figure 4A). Consistent with these changes in miR181b-3p expression, ethanol feeding also increased the expression of importin α5 in isolated non-parenchymal cells; this response was ameliorated by treatment with HA35 (Figure 4B). Immunohistochemical analysis was used to visualize the subcellular localization of phospho-p65 in the liver. After ethanol feeding, the nuclear localization of phosphorylated p65 was increased in both hepatocytes and non-parenchymal cells; this effect was normalized with HA35 treatment (Figure 4C).

Oral supplementation with HA35 reduced ethanol-induced injury in mouse liver

Since HA35 normalized cytokine responses in Kupffer cells from rats after ethanol feeding, as well as regulated the expression of miR181b-3p and importin α5 in mouse liver, we assessed the ability of HA35 to prevent ethanol-induced liver injury *in vivo.* Short-term ethanol increased AST in the circulation and HA35 treatment prevented this increase (Figure 5A). Ethanol consumption also increased hepatic steatosis as assessed by both biochemical measurement (Figure 5B) and neutral lipid staining using Oil Red O (Figure 5C). HA35 treatment did not prevent ethanol-induced steatosis (Figure 5B/C). Ethanol exposure also increased the expression of TNFα, IL-6, and MCP-1 mRNA in the liver (Figure 5D). HA35 treatment led to intermediate expression of TNFα mRNA and reduced expression of IL-6 and MCP-1 mRNA (Figure 5D). Short-term ethanol feeding also promoted apoptosis in the liver, assessed by enumerating TUNEL positive cells. TUNEL positive cells predominantly exhibited a morphology consistent with hepatocytes (Figure 6A). Accumulation of immunoreactive M30, the caspase cleavage product of cytokeratin-18, a hepatocyte-specific protein, was also increased by ethanol feeding (Figure 6B). HA35 treatment reduced both ethanol-induced TUNEL positive cells and M30 staining in the liver (Figure 6A/B).

HA35 maintains the intestinal barrier during ethanol-feeding

Since HA acts to improve gut barrier defenses via multiple mechanisms(13, 30) ((24), we investigated whether HA35 protected the gut from ethanol-induced injury. Ethanol feeding

increased endotoxin in the portal circulation, indicating a loss of gut integrity; this response was prevented by treatment of mice with HA35 (Figure 7A). Following short-term ethanol feeding, the co-localization of ZO-1 and occludin was disrupted in the proximal colon (Figure 7B). HA35 treatment prevented ethanol-induced disruption of ZO-1 and occludin co-localization at tight junctions; in HA35 treated/ethanol-fed mice, tight junction formation was comparable to pair-fed controls (Figure 7B). Neither ethanol exposure nor treatment with HA35 changed the expression of ZO-1, occludin or claudin 3 mRNA or protein (Supplemental Figure 3).

Discussion

Activation of innate immunity is a critical component in the development of ALD. Ethanol exposure not only increases the exposure of resident macrophages in the liver to PAMPs and DAMPs, it also sensitizes Kupffer cells to signaling via TLR4 ligands (4, 6). It has been our working hypothesis that therapeutic strategies that normalize, rather than completely inhibit, innate immune signaling are critical to the prevention and treatment of ALD. Here we have discovered that a small specific-sized HA of an average molecular weight of 35kD can normalize TLR4-mediated signaling in rat Kupffer cells from ethanol-fed rats. NGS of miRNAs down-regulated by ethanol, but restored by HA35, identified 3 miRNA involved in nuclear-cytoplasmic shuttling. Of these 3 miRNA, miR181b-3p, the miRNA that was most down-regulated by ethanol, was found to regulate the expression of importin α5, a protein involved in the shuttling of p65 to the nucleus. In an *in vivo* model of ethanol exposure, miR181b-3p was decreased in liver of ethanol-fed mice compared to pair-fed and treatment with HA35 prevented this decrease. Importin α5 expression in non-parenchymal cells was also reciprocally regulated by ethanol and HA35. Importantly, treatment of mice with HA35 was sufficient to prevent ethanol-induced liver injury and protect the barrier function of the intestine. Thus, these studies identify a miR181b-3p→importin-α5 axis that contributes to the ethanol-induced sensitization of inflammatory signaling pathways in hepatic macrophages (Figure 8).

HA is an abundant extracellular matrix component of vertebrates and is produced as a straight chain polymer strictly composed of repeating disaccharides of D-glucuronic acid and N-acetylglucosamine. HA is produced at cell surfaces by one or more plasma membrane embedded hyaluronan synthases (HAS1, HAS2 and HAS3). HA communicates with many cell types in a size-specific manner, using at least four signaling receptors including: 1) CD44, a ubiquitously-expressed cell surface protein that recognizes HA sizes greater than 8 sugar moieties in length (13); 2) RHAMM (receptor for HA mediated motility) which is important in signaling cell migration (13); and the TLR pattern recognition molecules 3)TLR4 and 4) TLR2 (10). The interaction of HA with receptors is thought to be size dependent. Specific-sized HA fragments recruit and activate leukocytes under pathological inflammatory settings and HA is now included among the DAMPs recognized in innate immunity (13). However, certain specific-sized HA fragments can also have protective, anti-inflammatory effects (31). Here we screened small specific-sized HA fragments, ranging from 7–74 kD, in an assay of TLR4-stimulated TNFα expression in Kupffer cells. While some of the small specific-sized HAs increased TNFα expression in Kupffer cells from pair-fed rats, none of the HAs increased expression in cells from ethanol-fed rats. It is likely that

the sensitization of TLR4 signaling due to ethanol exposure masked any DAMP-like activity of the HAs in Kupffer cells from ethanol-fed rats. Importantly, of all the fragments tested, only HA35 had anti-inflammatory effects. In parallel studies, we have identified CD44 as the critical receptor in mediating the anti-inflammatory effect of HA35 on Kupffer cells (Saikia, et al., manuscript submitted).

In order to better understand the mechanisms for both the sensitization of Kupffer cells to TLR4 signaling in response to ethanol and the protective effects of HA35, we carried out NGS of miRNAs from Kupffer cells from ethanol- and pair-fed rats, treated or not with HA35 *ex vivo.* Remarkably, this un-biased approach yielded 30 miRNAs that were reduced by ethanol, but only 3 of those miRNAs were restored with HA35. Targeted gene analysis identified these 3 reciprocally regulated miRNAs as regulators of nuclear-cytoplasmic shuttling. Interestingly, nuclear-cytoplasmic shuttling of HuR, an mRNA binding protein, is also disrupted by ethanol, leading to an increased accumulation of HuR in the cytosol which in turn stabilizes TNFα mRNA (32). In contrast to the role for importin-α5 in p65 translocation, HuR shuttling is dependent on chromosomal region maintenance protein (CRM1) (32). Taken together, these data suggest that nuclear-cytoplasmic shuttling may be an important target for normalizing the sensitization of TLR4 signaling in response to ethanol.

The role of miR181b-3p was investigated in more mechanistic detail. miR181b-3p expression was decreased both in Kupffer cells from ethanol-fed rats and in liver of mice after ethanol feeding. In both model systems, HA35 treatment restored miR181b-3p. Importin α5 was identified by bioinformatics as a target of miR181b-3p. Importin α5 is an importin α family member involved in the nucleocytoplasmic transport of cellular proteins expressing nuclear localization signals (28). Specifically, importin α5 is known to mediate translocation of NFκB subunits in leukocytes (29), thus integrating the effects of ethanol and HA35 on both NFκB signaling and nuclear-cytoplasmic shuttling. It is interesting to note that in both Kupffer cells and non-parenchymal cells isolated from mouse liver, the impact of ethanol on expression of importin α5 is approximately 2-fold, suggesting that the quantity of importin α5 in macrophages may limit p65 translocation under certain activation states.

The pathogenesis of ALD involves a dynamic interplay between the gut and liver, with ethanol exposure both impairing the intestinal barrier function and leading to dysbiosis (3). Interestingly, the protection observed with HA35 encompassed both intestinal and liver pathologies. Short-term ethanol feeding increased the concentration of portal endotoxin and disrupted epithelial tight junctions in the proximal colon, indicative of intestinal disruption. HA35 prevented ethanol-induced disruption of the barrier, maintaining the co-localization of ZO-1 and occludin at the paracellular junctions in the proximal colon and preventing ethanol-mediated increases in portal endotoxin. These responses are consistent with the protective effects of HA in both neonatal intestine and in response to injurious signals (4). HA is present in breast milk (16) and purified HA35 protects from *Salmonella* infection in human epithelium *in vitro* (18, 33). Treatment of mice with HA35 also increases expression of antimicrobial β-defensins in the intestinal epithelium (34). HA35 up-regulates ZO-1 in mice undergoing *Citrobacter rodentium* infection, associated with protection from *Citrobacter rodentium* infection *in vivo* (24). While our data from Kupffer cells indicates

that HA35 has direct effects on inflammatory signaling in Kupffer cells, it is also possible that HA35 treatment to mice during ethanol feeding has direct and/or indirect protective effects on the intestine. Dietary HA is absorbed and migrates to the skin and other organs, and is then excreted in the urine and feces (35). In differentiated Caco-2 monolayers, HA crosses the cell barrier in a size dependent manner, with smaller HA fragments having increased permeability (36). Radiolabeled HA studies in rats show that oral administration of HA lead to excretion in feces as well accumulation of HA in the skin with some residual in the blood up to 96 hours post treatment (37). However, the specific dynamics of HA35 absorption and metabolism are not well understood. Studies are currently underway to determine if HA35 can directly protect intestinal epithelial cells from challenge with ethanol, as well as to determine the pharmacodynamics of HA35 supplementation.

In summary, an un-biased analysis NGS data identified an important miR181b-3p→importin α5 regulatory axis in hepatic macrophages that contributed to the sensitization of Kupffer cells to TLR4-mediated cytokine production via enhanced accumulation of the p65 subunit of NFκB to the nucleus (Figure 8). Normalization of this miR181b-3p -importin α5 pathway by treatment of HA35, both in isolated Kupffer cells and in an *in vivo* model of ethanol-induced liver injury, protected from the effects of ethanol. Taken together, these data identify a novel pathway by which ethanol regulates innate immune activity, leading to the development of ethanol-induced liver injury.

Supplementary Material

Refer to Web version on PubMed Central for supplementary material.

Acknowledgments

Abbreviations

ALD	alcoholic liver disease
HA35	hyaluronic acid 35kD
miRNA	microRNA
LPS	lipopolysaccharide
PAMP	pathogen associated molecular pattern
DAMP	danger associated molecular pattern
NGS	next generation sequencing
RHAMM	receptor for HA mediated motility

CRM1 chromosomal region maitenance protein

References

Author names in bold designate shared co-first authorship

1. Gao B, Bataller R. Alcoholic liver disease: pathogenesis and new therapeutic targets. Gastroenterology. 2011; 141:1572–1585. [PubMed: 21920463]

2. Louvet A, Mathurin P. Alcoholic liver disease: mechanisms of injury and targeted treatment. Nat Rev Gastroenterol Hepatol. 2015; 12:231–242. [PubMed: 25782093]

3. Schnabl B, Brenner DA. Interactions between the intestinal microbiome and liver diseases. Gastroenterology. 2014; 146:1513–1524. [PubMed: 24440671]

4. Nagy LE. The Role of Innate Immunity in Alcoholic Liver Disease. Alcohol Res. 2015; 37:237–250. [PubMed: 26695748]

5. Petrasek J, Iracheta-Vellve A, Saha B, Satishchandran A, Kodys K, Fitzgerald KA, Kurt-Jones EA, et al. Metabolic danger signals, uric acid and ATP, mediate inflammatory cross-talk between hepatocytes and immune cells in alcoholic liver disease. J Leukoc Biol. 2015; 98:249–256. [PubMed: 25934928]

6. Dixon LJ, Barnes M, Tang H, Pritchard MT, Nagy LE. Kupffer cells in the liver. Compr Physiol. 2013; 3:785–797. [PubMed: 23720329]

7. Wu XQ, Dai Y, Yang Y, Huang C, Meng XM, Wu BM, Li J. Emerging role of microRNAs in regulating macrophage activation and polarization in immune response and inflammation. Immunology. 2016; 148:237–248. [PubMed: 27005899]

8. Szabo G, Satishchandran A. MicroRNAs in alcoholic liver disease. Semin Liver Dis. 2015; 35:36–42. [PubMed: 25632933]

9. Bala S, Marcos M, Kodys K, Csak T, Catalano D, Mandrekar P, Szabo G. Up-regulation of microRNA-155 in macrophages contributes to increased tumor necrosis factor {alpha} (TNF{alpha}) production via increased mRNA half-life in alcoholic liver disease. J Biol Chem. 2011; 286:1436–1444. [PubMed: 21062749]

10. Jiang D, Liang J, Noble PW. Hyaluronan in tissue injury and repair. Annu Rev Cell Dev Biol. 2007; 23:435–461. [PubMed: 17506690]

11. Karamanos NK, Linhardt RJ. Special issue: Proteoglycans: signaling, targeting and therapeutics: introduction. FEBS J. 2013; 280:2119. [PubMed: 23530537]

12. Tsutsumi M, Urashima S, Takase S, Ueshima Y, Tsuchishima M, Shimanaka K, Kawahara H. Characteristics of serum hyaluronate concentrations in patients with alcoholic liver disease. Alcohol Clin Exp Res. 1997; 21:1716–1721. [PubMed: 9438536]

13. Petrey AC, de la Motte CA. Hyaluronan, a crucial regulator of inflammation. Front Immunol. 2014; 5:101. [PubMed: 24653726]

14. Nakamura K, Yokohama S, Yoneda M, Okamoto S, Tamaki Y, Ito T, Okada M, et al. High, but not low, molecular weight hyaluronan prevents T-cell-mediated liver injury by reducing proinflammatory cytokines in mice. J Gastroenterol. 2004; 39:346–354. [PubMed: 15168246]

15. Muto J, Yamasaki K, Taylor KR, Gallo RL. Engagement of CD44 by hyaluronan suppresses TLR4 signaling and the septic response to LPS. Mol Immunol. 2009; 47:449–456. [PubMed: 19781786]

16. Kessler SP, Obery DR, de la Motte C. Hyaluronan Synthase 3 Null Mice Exhibit Decreased Intestinal Inflammation and Tissue Damage in the DSS-Induced Colitis Model. Int J Cell Biol. 2015; 2015:745237. [PubMed: 26448758]

17. de la Motte CA. Hyaluronan in intestinal homeostasis and inflammation: implications for fibrosis. Am J Physiol Gastrointest Liver Physiol. 2011; 301:G945–949. [PubMed: 21852366]

18. de la Motte CA, Kessler SP. The role of hyaluronan in innate defense responses of the intestine. Int J Cell Biol. 2015; 2015:481301. [PubMed: 25922605]

19. Thakur V, McMullen MR, Pritchard MT, Nagy LE. Regulation of macrophage activation in alcoholic liver disease. J Gastroenterol Hepatol. 2007; 22(Suppl 1):S53–56. [PubMed: 17567466]

20. Mandal P, Roychowdhury S, Park PH, Pratt BT, Roger T, Nagy LE. Adiponectin and heme oxygenase-1 suppress TLR4/MyD88-independent signaling in rat Kupffer cells and in mice after chronic ethanol exposure. J Immunol. 2010; 185:4928–4937. [PubMed: 20861358]

21. Cohen JI, Roychowdhury S, DiBello PM, Jacobsen DW, Nagy LE. Exogenous thioredoxin prevents ethanol-induced oxidative damage and apoptosis in mouse liver. Hepatology. 2009; 49:1709–1717. [PubMed: 19205032]

22. Barnes MA, McMullen MR, Roychowdhury S, Pisano SG, Liu X, Stavitsky AB, Bucala R, et al. Macrophage migration inhibitory factor contributes to ethanol-induced liver injury by mediating cell injury, steatohepatitis, and steatosis. Hepatology. 2013; 57:1980–1991. [PubMed: 23174952]

23. Roychowdhury S, McMullen MR, Pisano SG, Liu X, Nagy LE. Absence of receptor interacting protein kinase 3 prevents ethanol-induced liver injury. Hepatology. 2013; 57:1773–1783. [PubMed: 23319235]

24. Kim Y, Kessler SP, Obery DR, Homer CR, McDonald C, de la Motte CA. Hyaluronan 35kDa treatment protects mice from Citrobacter rodentium infection and induces epithelial tight junction protein ZO-1 in vivo. Matrix Biol. 2016

25. Hecker W, Witthauer D, Staerk A. Validation of dry heat inactivation of bacterial endotoxins. PDA J Pharm Sci Technol. 1994; 48:197–204. [PubMed: 7804819]

26. He X, Jing Z, Cheng G. MicroRNAs: new regulators of Toll-like receptor signalling pathways. Biomed Res Int. 2014; 2014:945169. [PubMed: 24772440]

27. Wong N, Wang X. miRDB: an online resource for microRNA target prediction and functional annotations. Nucleic Acids Res. 2015; 43:D146–152. [PubMed: 25378301]

28. Pumroy RA, Cingolani G. Diversification of importin-alpha isoforms in cellular trafficking and disease states. Biochem J. 2015; 466:13–28. [PubMed: 25656054]

29. Sun X, He S, Wara AK, Icli B, Shvartz E, Tesmenitsky Y, Belkin N, et al. Systemic delivery of microRNA-181b inhibits nuclear factor-kappaB activation, vascular inflammation, and atherosclerosis in apolipoprotein E-deficient mice. Circ Res. 2014; 114:32–40. [PubMed: 24084690]

30. Hill DR, Rho HK, Kessler SP, Amin R, Homer CR, McDonald C, Cowman MK, et al. Human milk hyaluronan enhances innate defense of the intestinal epithelium. J Biol Chem. 2013; 288:29090–29104. [PubMed: 23950179]

31. Cyphert JM, Trempus CS, Garantziotis S. Size Matters: Molecular Weight Specificity of Hyaluronan Effects in Cell Biology. Int J Cell Biol. 2015; 2015:563818. [PubMed: 26448754]

32. McMullen MR, Cocuzzi E, Hatzoglou M, Nagy LE. Chronic ethanol exposure increases the binding of HuR to the TNFalpha 3′-untranslated region in macrophages. J Biol Chem. 2003; 278:38333–38341. [PubMed: 12876290]

33. Riehl TE, Ee X, Stenson WF. Hyaluronic acid regulates normal intestinal and colonic growth in mice. Am J Physiol Gastrointest Liver Physiol. 2012; 303:G377–388. [PubMed: 22556141]

34. Hill DR, Kessler SP, Rho HK, Cowman MK, de la Motte CA. Specific-sized hyaluronan fragments promote expression of human beta-defensin 2 in intestinal epithelium. J Biol Chem. 2012; 287:30610–30624. [PubMed: 22761444]

35. Ivanov AI. Structure and regulation of intestinal epithelial tight junctions: current concepts and unanswered questions. Adv Exp Med Biol. 2012; 763:132–148. [PubMed: 23397622]

36. Hisada N, Satsu H, Mori A, Totsuka M, Kamei J, Nozawa T, Shimizu M. Low-molecular-weight hyaluronan permeates through human intestinal Caco-2 cell monolayers via the paracellular pathway. Biosci Biotechnol Biochem. 2008; 72:1111–1114. [PubMed: 18391466]

37. Oe M, Mitsugi K, Odanaka W, Yoshida H, Matsuoka R, Seino S, Kanemitsu T, et al. Dietary hyaluronic acid migrates into the skin of rats. Scientific World Journal. 2014; 2014:378024. [PubMed: 25383371]
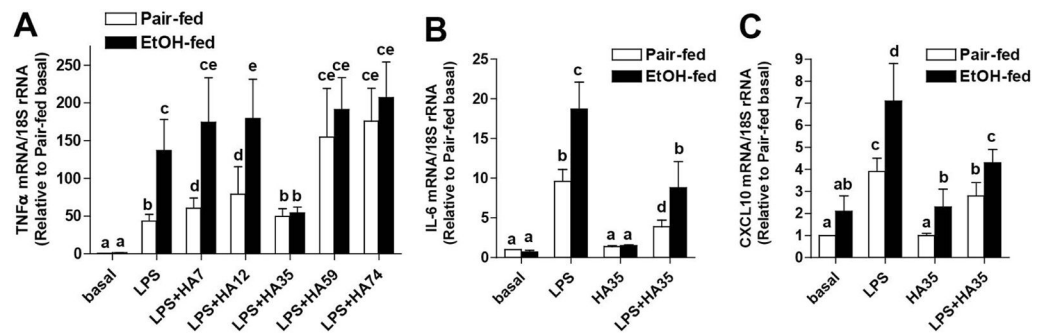
Figure 1. Small specific-sized HA differentially influence LPS-stimulated cytokine expression in primary cultures of rat Kupffer cells from ethanol- and pair-fed rats

Wistar rats were allowed free access to a Lieber-DeCarli ethanol diet or pair-fed control diet for 4 weeks. Kupffer cells were isolated and cultured overnight. Kupffer cells were then treated with 100μg/ml specific-sized HA fragments for 5h and then challenged with 10ng/ml LPS for an additional 1hr. Expression of TNFα **(A)**, IL6 **(B)** and CXCL10 **(C)** mRNA was measured by qRT-PCR and normalized to 18S rRNA. **(A)** n=10–14 and **(B/C)** n=4–5.
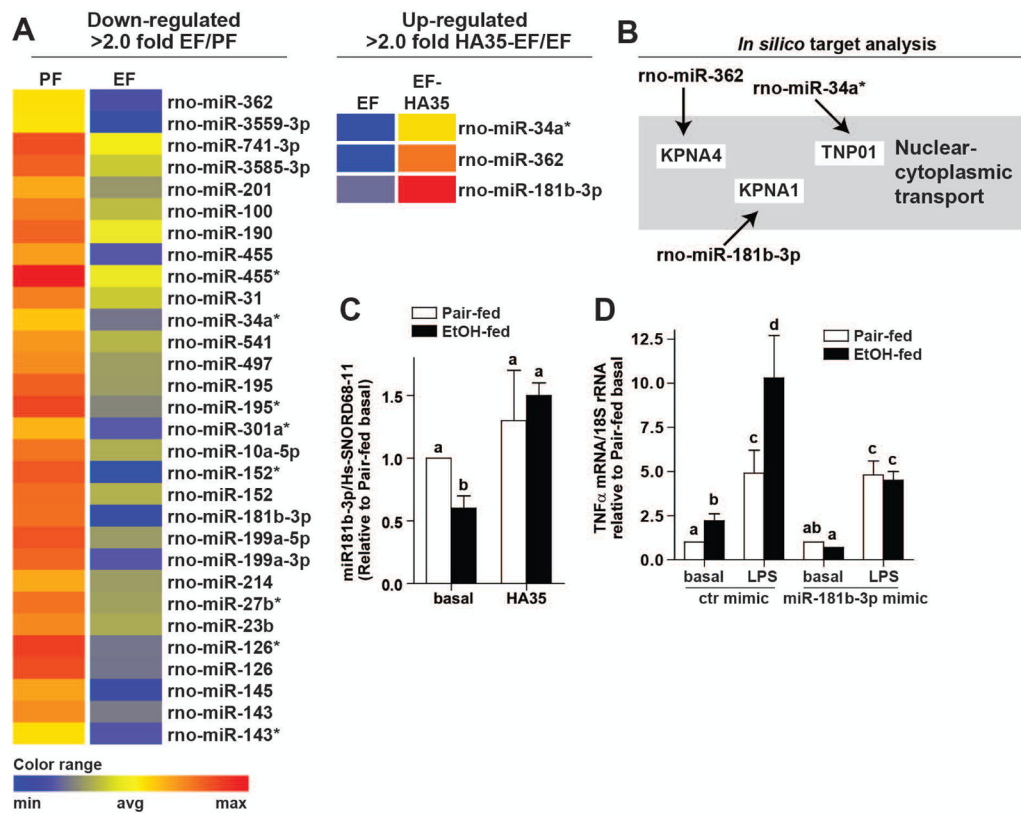
Figure 2. Next Generation Sequencing identifies miR181b-3p as a negative regulator of LPS-stimulated TNFα in Kupffer cells from ethanol-fed rats

(**A**) miRNA isolated from Kupffer cells from ethanol- and pair-fed rats treated or not with 100μg/ml HA35 for 5 h was analyzed by NGS. Heat maps illustrate the changes in expression for the 30 miRNAs identified whose expression was decreased by more than 2-fold by ethanol feeding. Of these thirty miRNA, heat maps are shown for the 3 miRNA whose expression was restored by treatment with HA35. Fold changes are shown in Supplemental Tables 2 and 3. (**B**) Cartoon illustrates an *in silico* gene targeting analysis identifying nuclear-cytoplasmic shuttling as a common target of the three reciprocally regulated miRNA. (**C**) Kupffer cells isolated from ethanol- and pair-fed rats were treated or not with HA35 for 5 h. Expression of miR181b-3p was measured by qRT-PCR and normalized to Hs-SNORD68-11. (**D**) Kupffer cells were nucleofected with either control miRNA mimic or miR181b-3p mimic. 18hr post-nucleofection, Kupffer cells were challenged with 10ng/ml LPS for 1 hr and expression of TNFα mRNA measured by qRT-PCR and normalized to 18S rRNA. n=4.
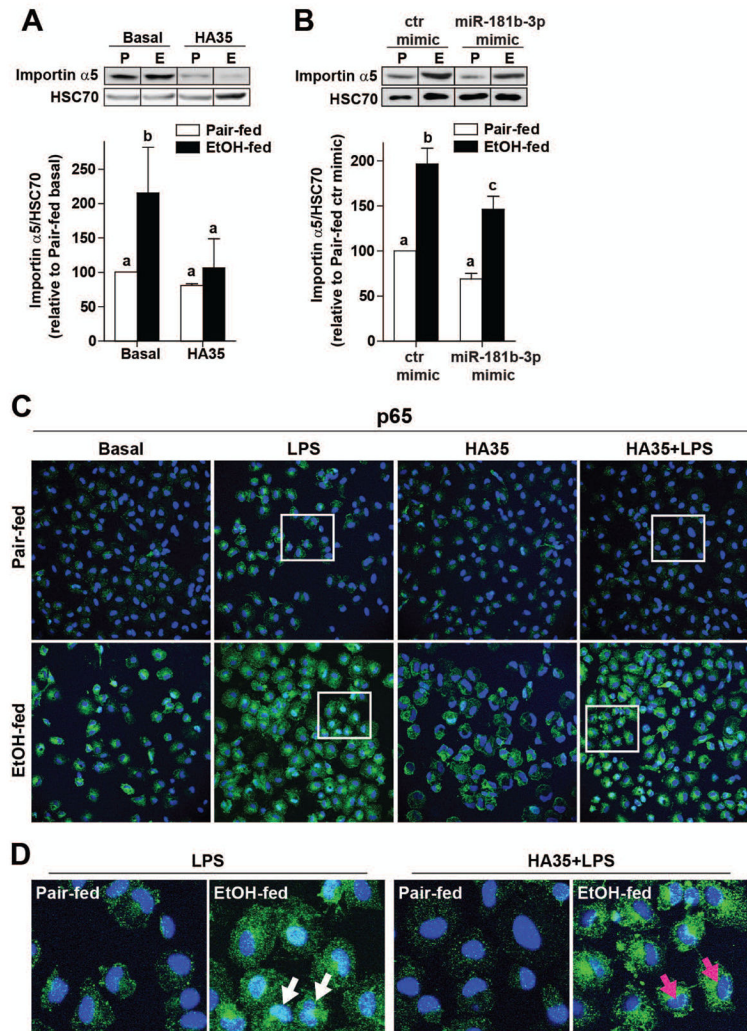
Figure 3. Regulation of importin α5 expression by ethanol and miR181b-3p impacts the nuclear translocation of the p65 subunit of NFκB in primary Kupffer cells

Kupffer cells isolated from ethanol- and pair-fed rats were **(A)** treated with 100μg/ml HA35 for 5 h or **(B)** nucleofected for 18 h with either control miRNA mimic or miR181b-3p mimic. **(A/B)** Kupffer cells were lysed and importin α5 expression measured by Western blot. HSC70 was used as a loading control. Images were cropped for representational purposes. n=4 independent Kupffer cell isolations. **(C)** The subcellular localization of p65 subunit of NFκB was assessed by confocal microscopy. Kupffer cells isolated from ethanol- and pair-fed rats were treated or not with HA35 for 5 h and then challenged with 10ng/ml LPS for 30 min. Cells were labeled with antibody to p65 and nuclei visualized with DAPI. **(D)** Zoomed images at the bottom of the panel illustrate Kupffer cells treated with LPS. White arrows point to p65 co-localized with DAPI and magenta arrows show nuclei only stained with DAPI. Images are representative of 4 independent Kupffer cell isolations.
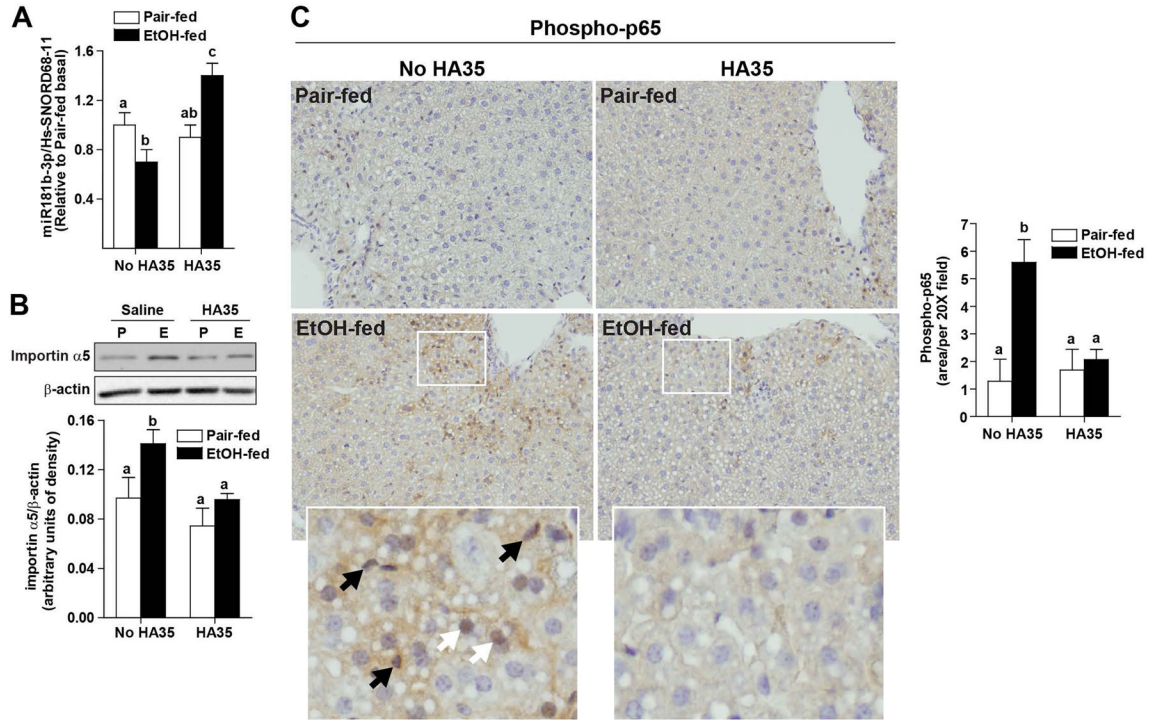
Figure 4. Regulation of importin α5 expression by ethanol and HA35 in an *in vivo* mouse model of ethanol-induced liver injury

C57BL/6J mice were allowed free access to an ethanol containing diet for 4 days (2 days at 1% (v/v) ethanol, followed by 2 days 6% (v/v) ethanol) or pair-fed an isocaloric control diet. Mice were gavaged once daily for the last 3 days of ethanol feeding with HA35 at 1.5mg/kg body weight or saline control the last three days of the study. **(A)** Expression of miR181b-3p in whole liver was determined by qRT-PCR and normalized to Hs-SNORD68-11. **(B)** Non-parenchymal cells were isolated from livers by collagenase digestion and differential centrifugation. Cells were lysed and expression of importin α5 measured by Western blot and normalized to β-actin. **(A–B)** n=4 pair-fed and n=5–6 ethanol-fed. **(C)** Formalin-fixed paraffin-embedded sections of liver were de-paraffinized and localization of phospho-p65 was assessed by immunohistochemistry. Images were acquired at 20X. Black arrows on zoomed insets identify phospho-p65 in non-parenchymal cells while white arrows indicate hepatocytes. Images are representative of duplicate images from 4 pair-fed and 5–6 ethanol-fed mice in each treatment group.
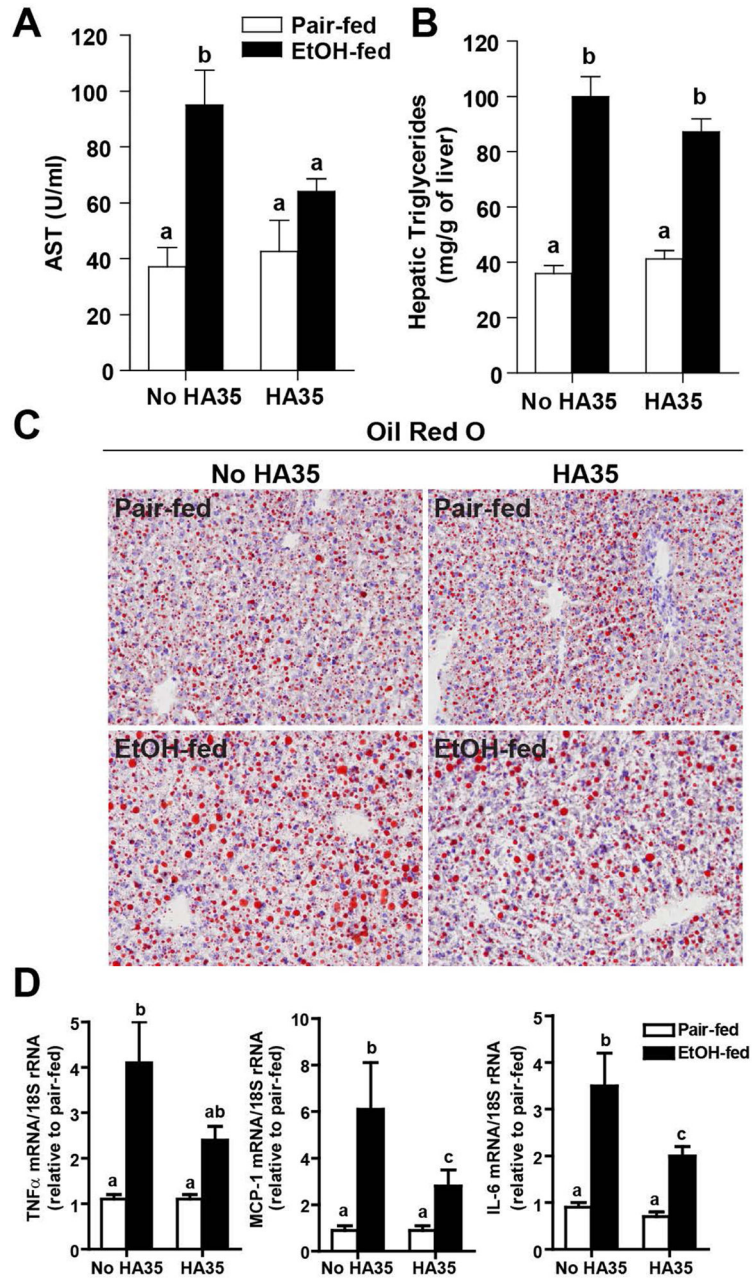
Figure 5. HA35 treatment reduces ethanol-induced liver injury

C57BL/6J mice were allowed free access to an ethanol containing diet for 4 days and treated or not with HA35, as described in Fig 4. **(A)** Plasma AST activity was measured by enzymatic assay. **(B)** Hepatic triglycerides were measured by biochemical assay. **(C)** Frozen liver sections were stained with Oil-Red O to visualize neutral lipids. Images acquired at 20X magnification. **(D)** Expression of IL-6, TNFα and MCP-1 mRNA was determined by qRT-PCR and normalized to 18S. For pair-fed n=4 **(A–C)** and 7–8 **(D)** and for ethanol-fed n=6 **(A–C)** and 10–11 **(D)**.
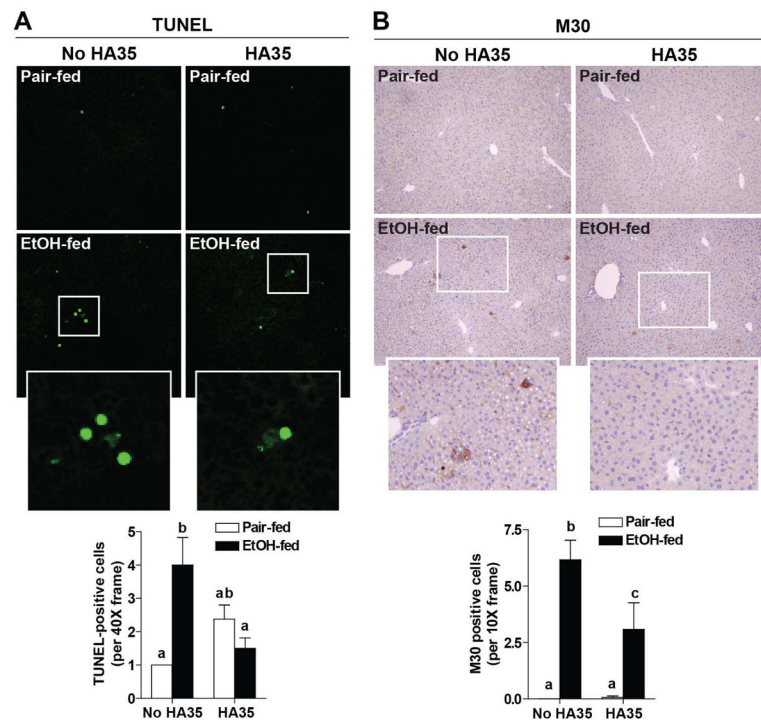
Figure 6. HA35 prevents ethanol-induced increases in apoptosis of hepatocytes
C57BL/6J mice were allowed free access to an ethanol containing diet for 4 days and treated or not with HA35, as described in Fig 4. Paraffin-embedded liver sections were de-paraffinized and followed by **(A)** TUNEL or **(B)** M30 immunostaining. TUNEL or M30 positive cells were manually counted per 40X or 10X field, respectively. n=4 pair-fed and n=6 ethanol-fed.
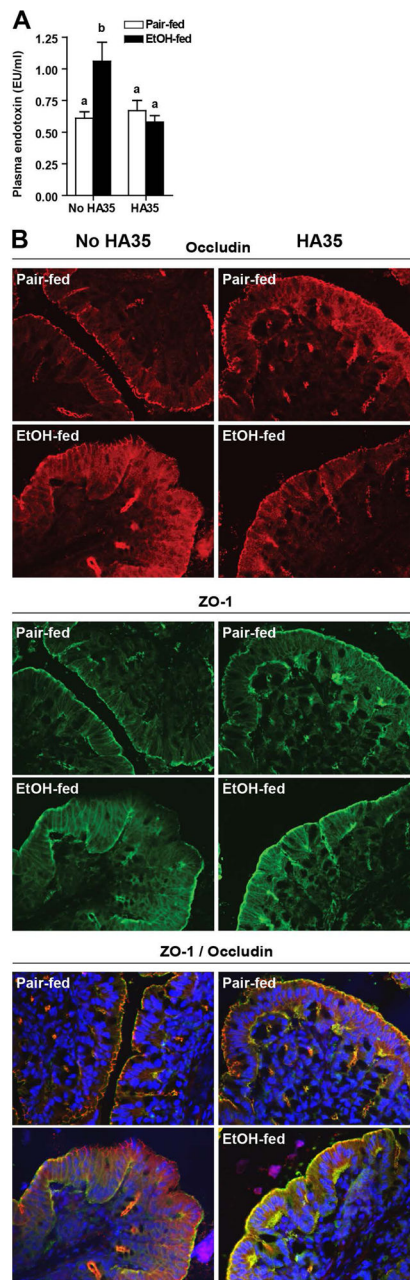
Figure 7. HA35 feeding prevents ethanol-induced disruption of the intestinal barrier
C57BL/6J mice were allowed free access to an ethanol containing diet for 4 days and treated or not with HA35, as described in Fig 4. **(A)** Plasma endotoxin was measured from portal blood. **(B)** Immunostaining for ZO-1 (green) and occludin (red) in de-paraffinized sections of proximal colon fixed with HistoChoice. Nuclei were stained using DAPI (blue) as a counterstain. Images were acquired at 40X magnification and are representative of n=3–4 for pair-fed and n=5 for ethanol-fed. For pair-fed n=6–7 **(A)** and 3–4 **(B)** and for ethanol-fed n=11 **(A)** and 5 **(B)**.
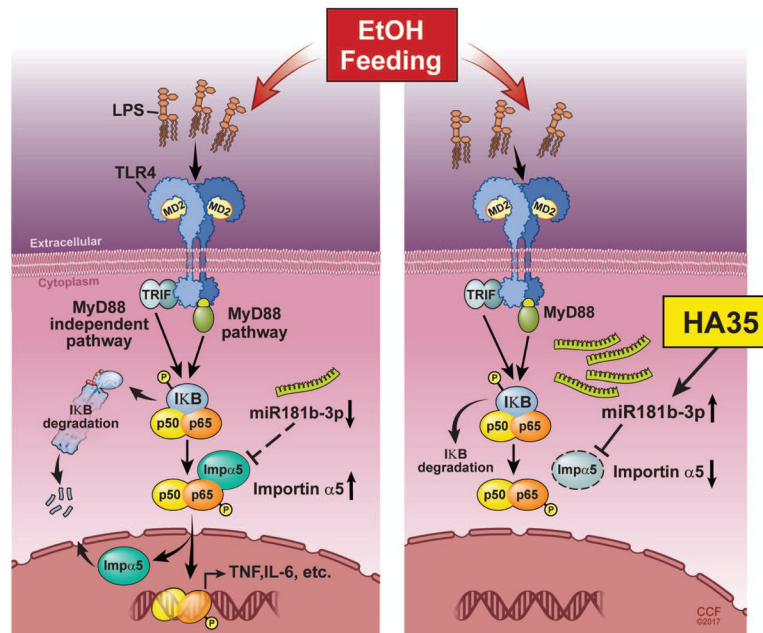
Figure 8. Model illustrating the interactions between ethanol and H35 on miR181b-3p and importin α5

Ethanol exposure decreases the expression of miR181b-3p which in turn results in increased expression of importin α5. Increased importin α5 allows for increased translocation of p65 to the nucleus, contributing to increased cytokine expression in Kupffer cells. Treatment with HA35 normalizes the expression of miR181b-3p and importin α5, as well as the sensitivity of Kuppfer cells to TLR4-mediated cytokine expression.